Indonesian Journal of Maritime Technology (ISMATECH)
Vol. 04, Issue 01, June 2026
eISSN: 3025-518X
DOI: https://doi.org/10.35718/ismatech.v4i1.8481997

Resistance Analysis for the Application of Flowbow on DTMB 5415 Ship

Arga Setya Andeardani[1], I Ketut Suastika[1*], Baharuddin Ali[2], Taufiq Arif Setyanto[2], Mahendra Indiaryanto[2], Amalia Ika Wulandari[3], Anson Novendra Pradana[4]

[1]Department of Naval Architecture, Sepuluh Nopember Institute of Technology (ITS) , Surabaya, 60117, Indonesia
[2]Research Center for Hydrodynamics Technology, BRIN, Surabaya, 60117, Indonesia
[3]Department of Naval Architecture, Kalimantan Institute of Technology, Balikpapan, 76127, Indonesia
[4]Department of Hull Form Development, West Japan Fluid Engineering Laboratory CO., LTD. Japan

KEYWORDS
Resistance;
Bulbous bow;
Flowbow;
CFD;
Semi-Displacement

ABSTRACT – Flowbow is an innovation designed by Rasmussen to increase fuel efficiency by reducing wave making resistance of ship. It is claimed that Flowbow can reduce the resistance of displacement and semi-displacement hull type at Froude number (Fr) over 0.25 to 0.28. On a warship, resistance reduction can increase the patrolling endurance by reducing energy used for moving. This research compares the hull of DTMB 5415 model, which is already using bulbous bow and the modified DTMB 5415 hull with the addition of Flowbow using CFD which is validated by EFD. The results show that the addition of a Flowbow reduces ship resistance at Fr greater than 0.249 and the resistance reduction increases as the ship speed increases. At the highest tested speed (Fr = 0.352), the total resistance reduction reaches 8.57%.

*Corresponding Author | I Ketut Suastika | ✉ (suastika@its.ac.id)

INTRODUCTION

Bow is the part of the ship that most affects the resistance it receives. The shape of the bow [1] and the angle of attack [2] significantly influence the resistance encountered, so the bow must be designed to optimize hydrodynamic performance. Bulbous-bow are structural additions to the bow designed to reduce wave drag by generating waves that interfere with those that would otherwise form at the ship's bow. Bulbous-bows can reduce wave drag by up to 5–15% of the ship's total drag at specific design speeds [3].

The effectiveness of a bulbous bow is influenced by the suitability of its design to the ship's operating conditions, particularly the Froude number and design speed. The effectiveness of a bulbous bow is greatly influenced by the suitability of its design to the ship's operating conditions, particularly the Froude number and design speed. Recent studies indicate that optimizing the bulb's shape using CFD methods can enhance destructive wave interference, thereby significantly reducing drag. Research [4] shows that variations in bulb geometry can reduce drag by more than 10%, while the influence of operating conditions such as draft and trim [5]. Additionally, RANS approach in CFD provides accurate predictions for drag analysis and bow design optimization [6].

Parallel with these developments, various alternative bow design innovations have begun to emerge as efforts to improve hydrodynamic performance beyond the conventional bulbous bow concept. FlowBow® serves the same function as a bulbous bow; what sets it apart is its shape and mechanism of operation. FlowBow® is shaped like a foil that works by directing the water flow vertically along the shape of the foil, which reduces wave resistance. The reduction in ship resistance applies at speeds above a Froude number (Fr) of 0.25–0.28 [7]. However, there have not been many studies examining FlowBow.

On large combat vessels such as destroyers, which typically have a semi-displacement hull, reducing drag is essential because it directly affects the vessel's energy efficiency and range. Research shows that drag reduction on the DTMB 5415 semi-displacement ship can be achieved by modifying the bulbous bow shape [8]. However, there has been no research specifically comparing the performance of the bulbous bow and FlowBow® on semi-displacement ship models such as the DTMB 5415, nor has there been a study testing the application of FlowBow® on combat ships.

With the development of technology, Computational Fluid Dynamics (CFD) allows ship resistance analysis to be conducted without physical testing in a towing tank. However, validation of the CFD results is still necessary. Based on this, this study aims to analyze the effect of applying FlowBow® on the resistance of the DTMB 5415 ship, which already has a bulbous bow, and to validate the CFD simulation results using experimental data. The study was conducted at several speed variations, neglecting the effects of stability, trim, and sinkage.

METHODS

This study employs a quantitative research design based on numerical simulation using a CFD approach conducted with Ansys Fluent. The computational approach utilizes the Reynolds-Averaged Navier–Stokes (RANS) equations with the k-ω SST turbulence model. The research design is comparative, analyzing two models: the DTMB 5415 vessel without bow modifications and the same vessel with the addition of a Flowbow.

Governing Equations

RANS is a turbulent flow model commonly used in CFD. RANS offers the advantage of lower computational costs compared to other methods [9]. The RANS equations are shown in Equations (1) and (2).
Continuity equations

$$\nabla . [\rho\, U] = 0 \tag{1}$$

Momentum equation

$$\frac{\partial[\rho U]}{\partial t} + \nabla \cdot \{\rho UU\} = -\nabla P + [\nabla \cdot [\tau\, ij - \rho u'u]] + \rho\, g' \tag{2}$$

The turbulence model is based on k-ω SST (Shear-Stress Transport) due to its ability to accurately simulate both near-wall and far-wall flow [10]. This model includes two transport equations: the turbulent kinetic energy (k) and the turbulent frequency (ω). The turbulent viscosity value is obtained using Equation (3).

$$\mu_t = \frac{\rho k}{\omega} \frac{1}{\max\left(\frac{1}{\alpha^*}, \frac{SF_2}{a_1 \omega}\right)} \tag{3}$$

Modelling

The geometric design was based on the linesplan data for vessel DTMB 5415 that obtained from sinman website, which is also used by BRIN for EFD test.

Table 1. Dimention of DTMB 5415

Item	Symbol	Model	Unit
Length Between Perpendicular	LPP	5,719	m
Length Waterline	LWL	5,726	m
Breath Moulded	B	0,768	m
Draught	T	0,248	m
Displacement	Δ	0,551	ton
Wetted Surface Area	WSA	4,786	m^2

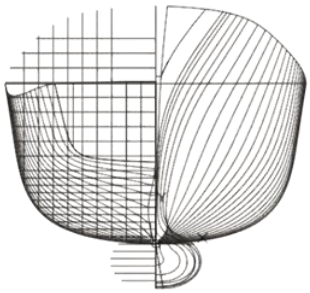

Figure 1. Lines plan of DTMB 5415

Modeling was performed using Maxsurf Modeller software. The results were then exported to a 3D CAD program to convert the ship model into a solid model. Once converted to a solid model, it was saved in Parasolid format (.x_t).

Figure 2. Used 3D model of DTMB 5415

The DTMB 5415 model was created based on the model used in the EFD testing by BRIN. A comparison between the DTMB 5415 model and the EFD model can be considered valid if the difference is less than 2% [11].

Table 2. Dimention comparation between model of DTMB 5415 used for CFD and EFD

Item	Model		Difference	unit
	EFD	CFD		
LPP	5.719	5.719	0.00%	m
LWL	5.726	5.726	0.00%	m
B	0.768	0.768	0.00%	m
T	0.248	0.248	0.00%	m
Δ	0.551	0.552	0.10%	ton
WSA	4.786	4.786	0.00%	m^2

The design of the DTMB 5415 with FlowBow® was achieved by modifying the bow shape and adapting it to the FlowBow® foil profile. Based on the FlowBow® patent, the FlowBow® application consists of the FlowBow® body and a V-wedge that connects the body to the ship's hull. The DTMB 5415 model with FlowBow® has the same displacement volume as the DTMB 5415 model.

Table 3. Dimension comparation between DTMB 5415 and modified DTMB 5415 model with Flowbow added

Dimension	Bulbous bow	Flowbow	Unit	Difference
Lwl	5.719	5.727	m	-0.14%
∇	0.552	0.557	m^3	-0.91%
Δ	0.552	0.557	ton	-0.91%
WSA	4.786	5.022	m^2	-4.93%

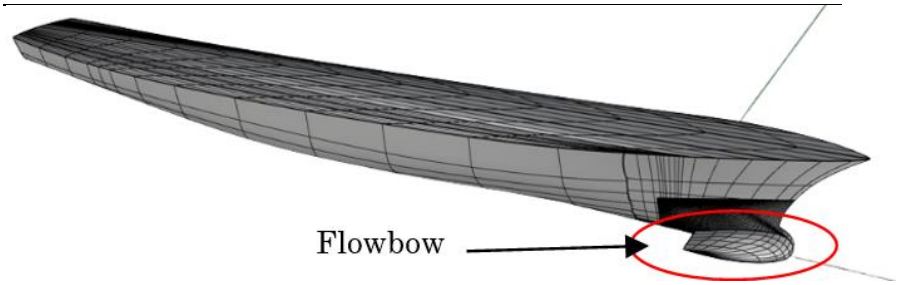

Figure 3. Modified DTMB 5415 with Flowbow added

Simulation Set Up

The simulation was conducted using Ansys Fluent software. The simulation process involved creating the simulation domain, meshing, configuring the setup, and running the simulation. The simulation domain was created in accordance with the ITTC guidelines for CFD simulations [12]. The dimensions and boundary conditions of the simulation domain are shown in Figure 4 and Table 4.

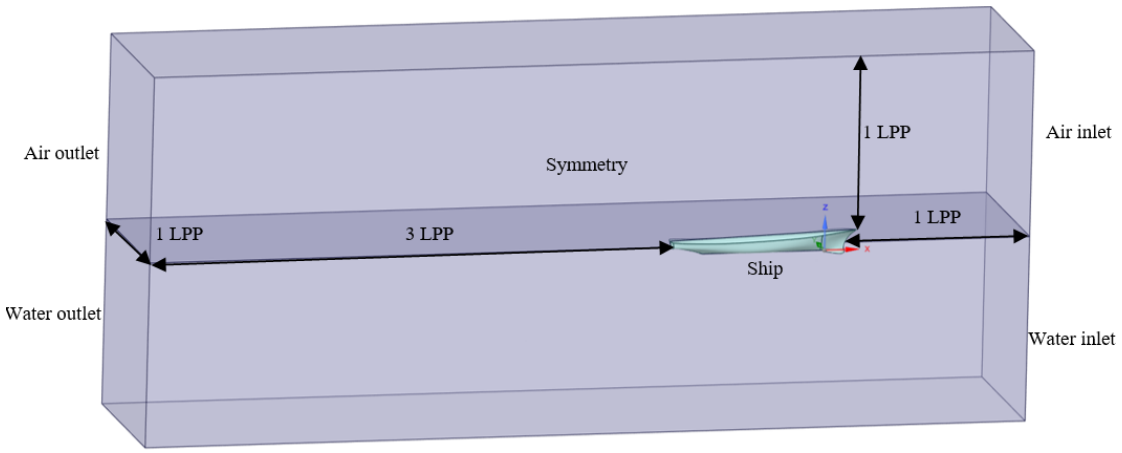

Figure 4. Named selection of boundary condition

Table 4. Type of boundary condition

Name Selection	Boundary type
Air inlet	Velocity Inlet
Water Inlet	Velocity Inlet
Air outlet	Pressure Outlet
Water outlet	Pressure Outlet
Ship	Wall
Symmetry	Symmetry
Top	Symmetry
Bottom	Symmetry
Side	Symmetry

The meshing process was conducted using local sizing on the ship's surface and the body of influence located 500 mm from the water surface. The mesh employs a shared topology to connect the air and water domains. In simulations using the K-ω SST model, the boundary layer is required to have a Y^+ value below 1 or within the range of 30–300. This simulation was conducted using a Y+ value of 95. Figure 5 shows the meshing of DTMB 5415 model.

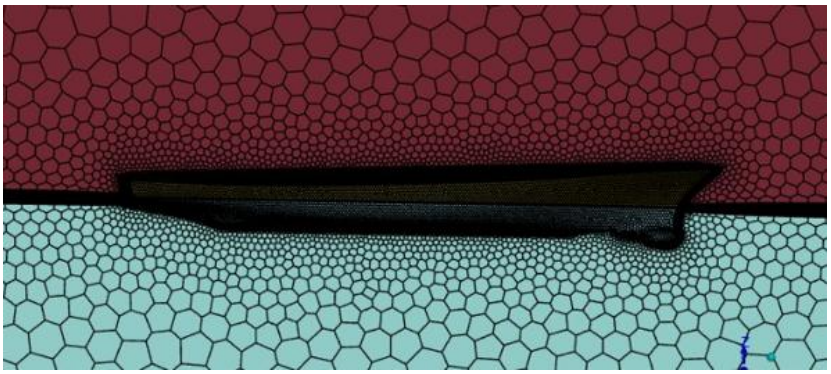

Figure 5. Meshing of DTMB 5415 model

The simulation setup included a pressure-based solver with steady flow and gravity aligned with the ship's vertical axis. The materials used in this simulation were air and freshwater (liquid H_2O). The simulation was performed using a multiphase volume-of-fluid (VOF) simulation model and a turbulence model based on the RANS Equations with k-ω SST.

The velocity variations are based on tests conducted by BRIN on the DTMB 5415 model. The velocity variations used are shown in Table 5:

Table 5. Model speed

Fr	Speed (m/s)
0.198	1.483
0.249	1.866
0.280	2.096
0.300	2.251
0.352	2.636

RESULTS AND DISCUSSION

The CFD simulations were validated using grid independence tests (GI), grid convergence tests (GCT), and a comparison of the results with EFD simulations. The EFD to CFD validation tests were performed on the DTMB 5415 model. The validated results were then used to compare the simulation results of the DTMB 5415 models with added Flowbow modifications.

Grid Independence Test

A grid independence test was conducted to determine the appropriate number of elements in the CFD simulation to ensure the results are valid. The simulation was conducted repeatedly by increasing the number of mesh elements for each iteration until the difference in results was insignificant [13], approximately less than 2% [14]. The results of the grid independence test for the original DTMB 5415 model are shown in Table 6 and Figure 6.

Table 6. Grid independence test of DTMB 5415 model

Cell	Resistance (N)	Difference
170698	76.911	
238050	78.78	-2.46%
307320	79.504	-0.89%
496358	79.665	-0.20%
619427	79.886	-0.28%

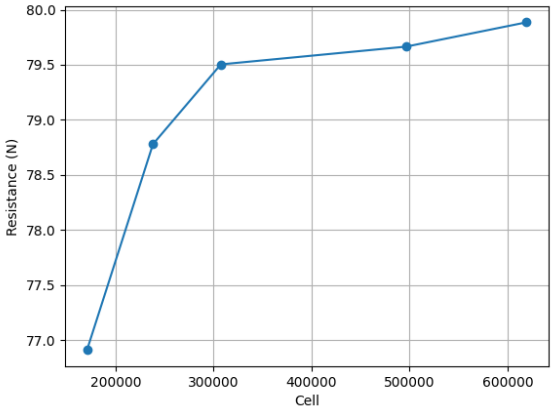

Figure 6. Grid Independence Test of DTMB 5415 Model

The results of the GI test for the DTMB model using FlowBow® are shown in Table 7 and Figure 7.

Table 7. Grid independence test of modified DTMB 5415with Flowbow model

Cell	Resistance (N)	Difference
200655	79.48	
559227	76.002	4.38%
920013	74.524	2.57%
1730066	72.834	1.65%
2941451	72.734	0.14%

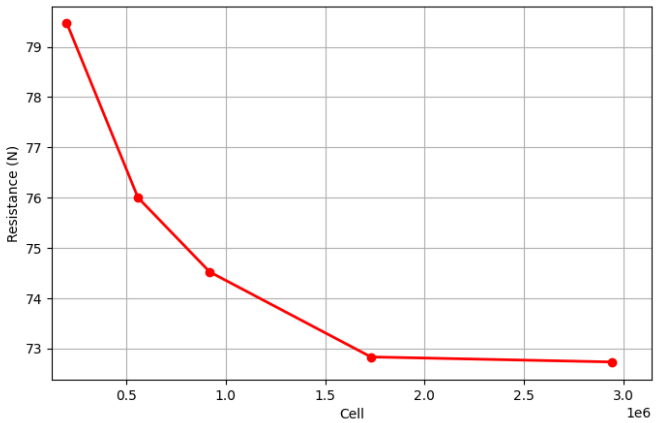

Figure 7. Grid Independence Test of Modified DTMB 5415with Flowbow Model

Grid Convergence Test

A grid convergence test is used to determine the uncertainty of the mesh used in the simulation [15]. In this process, three mesh variants of different quality are compared. The GCT calculations follow the method described by Celik [16].

The results of the grid convergence test for the DTMB 5415 model and Flowbow added DTMB 5415 model are shown in Table 8.

Table 8. Grid Convergence Test Result

Output	Equation	DTMB	Flowbow
Difference of Estimation	$\varepsilon_{21} = T_2 - T_1$	0.08	-0.10
	$\varepsilon_{32} = T_3 - T_2$	0.11	-1.22
Convergence Ratio	$R_i = \frac{\varepsilon_{21}}{\varepsilon_{32}}$	0.73	0.08
Grid Refinement Factor	$ri = \left(\frac{T_3}{T_1}\right)^{-1/3}$	1.26	1.47
Accuration Order	$p = \frac{\ln R_i}{\ln r_i}$	1.35	6.46
Extrapolated Value	$T_{ext21} = \frac{(r_{21}{}^p \times T1) - T2}{(r_{21}{}^p - 1)}$	39.53	74.16
	$T_{ext32} = \frac{(r_{32}{}^p \times T2) - T3}{(r_{32}{}^p - 1)}$	39.53	72.84
Estimated relative difference	$ea_{-21} = \left\|\frac{(T_1 - T_2)}{T_1}\right\|$	0.203%	1.646%
	$ea_{-32} = \left\|\frac{(T_2 - T_3)}{T_2}\right\|$	0.277%	0.137%
Extrapolated relative difference	$e_{ext-21} = \left\|\frac{(T_{ext-21} - T_1)}{T_{ext-21}}\right\|$	0.548%	0.147%
	$e_{ext-32} = \left\|\frac{(T_{ext-32} - T_2)}{T_{ext-32}}\right\|$	0.750%	0.012%
Grid Convergence Index	$GCI_{21} = \frac{Fs \cdot ea_{21}}{(R_{21}{}^p - 1)}$	0.685%	0.184%
	$GCI_{32} = \frac{Fs \cdot ea_{32}}{(R_{32}{}^p - 1)}$	0.937%	0.015%

Comparative Validation of CFD Using EFD

The DTMB model utilized in the CFD simulation is derived from a model previously tested for resistance in a towing tank by BRIN. The discrepancy in drag results between the experimental fluid dynamics (EFD) measurements and the CFD simulation is deemed acceptable, with an error range of 1% to 5% [17]. A comparative analysis of the CFD and EFD results is presented in Table 9.

Table 9. CFD Comparative Validation Using EFD

Fr	RT (N)		Difference
	EFD	CFD	
1.483	23.286	22.363	3.96%
1.866	34.948	35.071	-0.35%
2.096	45.63	45.74	-0.24%
2.251	55.526	54.327	2.16%
2.636	81.53	79.665	2.29%

Simulation Result Comparation

The comparison of the total resistance coefficient (c_T) between DTMB 5415 ship model with DTMB 5415 modified with FlowBow® is shown into table 10.

Table 10. Total resistance coefficient between models

SPEED		C_T		Difference
m/s	Fr	Flowbow	DTMB	
1.483	0.198	0.0053	0.0042	31.37%
1.866	0.249	0.0042	0.0042	4.86%
2.096	0.28	0.0041	0.0044	-2.27%
2.251	0.30	0.0042	0.0045	-2.71%
2.636	0.352	0.0042	0.0048	-8.57%

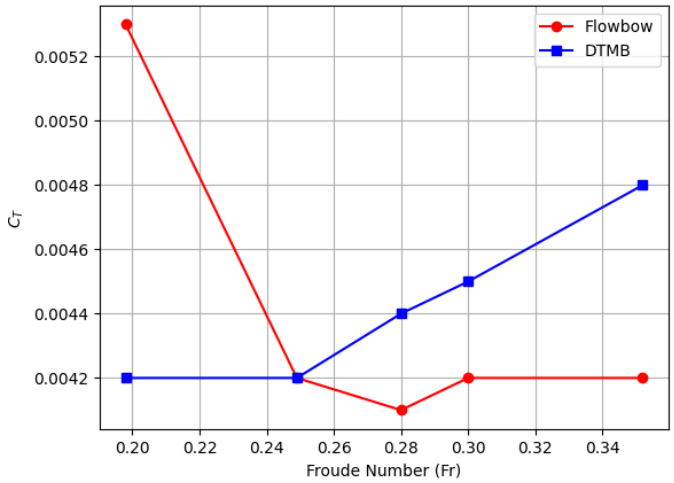

Figure 8. Total Resistance Coefficient Comparation

As shown in Figure 8, both models have the same C_T at Fr = 0.249, indicating equal overall resistance at this speed. At higher speed, the FlowBow® configuration shows lower C_T values, indicating reduced total resistance compared to the original DTMB 5415 hull. To evaluate the effect of FlowBow® on wave resistance, the total resistance is decomposed into the viscous resistance coefficient (Cv) and the wave resistance coefficient (Cw).

Table 11. Pressure Resistance Coefficient and Viscous Resistance Coefficient Between Models

SPEED		*VISCOUS*		*PRESSURE*	
(m/s)	Fr	FlowBow®	DTMB 5415	FlowBow®	DTMB 5415
1.483	0.198	0.0032	0.0031	0.0021	0.0012
1.866	0.249	0.0029	0.0030	0.0013	0.0012
2.096	0.280	0.0028	0.0029	0.0012	0.0014
2.251	0.300	0.0028	0.0029	0.0014	0.0016
2.636	0.352	0.0027	0.0028	0.0015	0.0020

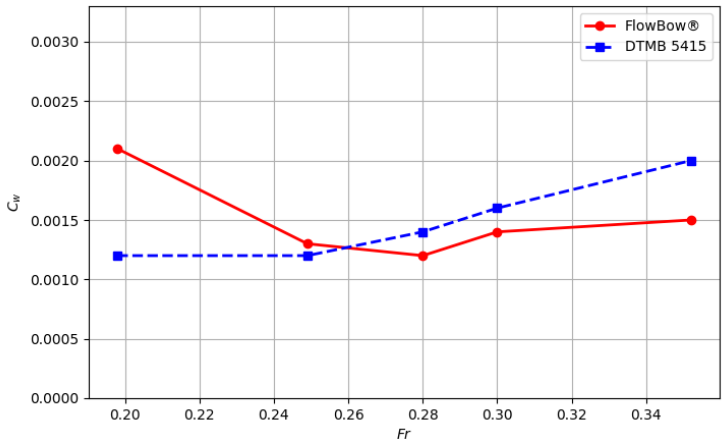

Figure 9. Pressure Resistance Coefficient Comparation

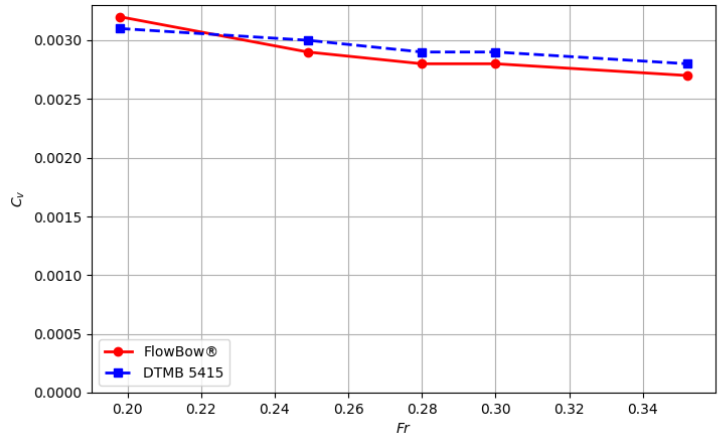

Figure 10. Viscous Resistance Coefficient Comparation

A comparison between Figures 9 and 10 suggests that Flowbow® influences wave making resistance. It is observed that for Fr below 0.258, Flowbow® leads to an increase in wave resistance. In contrast, beyond Fr = 0.258, higher velocities result in greater reductions in wave resistance.

Flow Analisys

To compare the flow conditions between a bulbous bow and a FlowBow®, visualizations of dynamic pressure contours were used. The following figure shows a comparison of these dynamic pressure contours on the highest tested speed (Fr = 0.352).

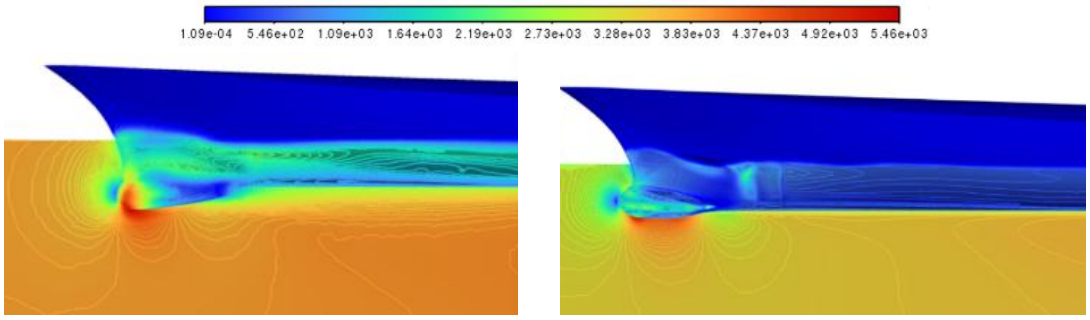

Figure 11. Dynamic Pressure Contours at the Highest Tested Speed (Fr = 0.352) for the Bulbous Bow (left) and FlowBow® (right).

As shown in Figure 11, there is a clear difference between the two configurations. On the DTMB 5415 with a conventional bulbous bow, the high-pressure area at the bow is wider and concentrated near the front, as shown in Figure 11 (left). This concentrated pressure indicates increased wave-making resistance, resulting in

higher power requirements to maintain the ship's speed. In contrast, the FlowBow® configuration shows a narrower high-pressure region that dissipates more rapidly along the hull, as shown in Figure 11 (right). This indicates reduced wave formation and a more efficient distribution of flow energy. This effect is further enhanced by the formation of flow channels that accommodate the vertical displacement of water masses driven by the FlowBow®.

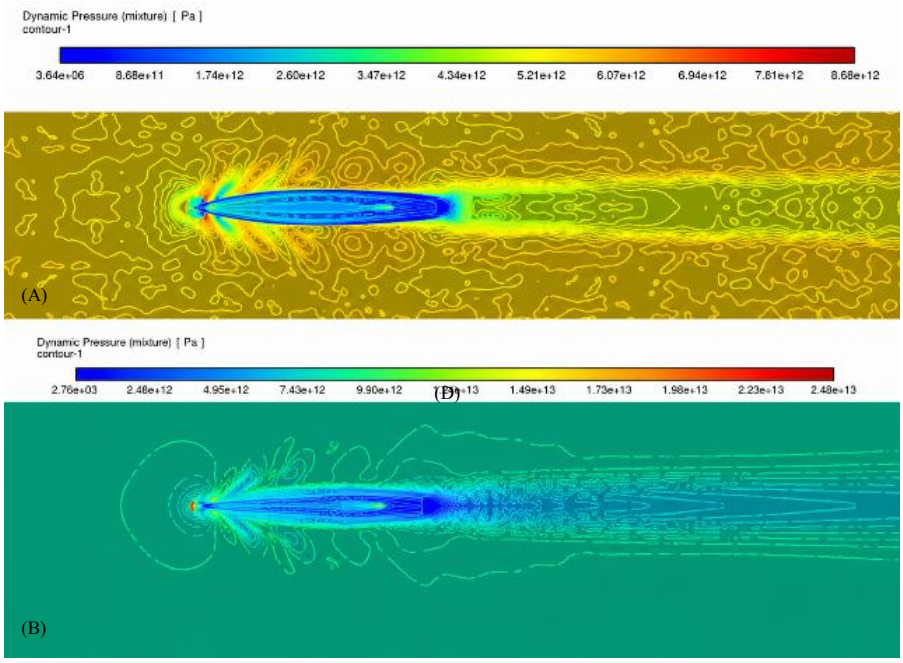

Figure 12. Wave Contour Distributions at Two Froude Numbers for Different Bow Configurations: (a) FlowBow® at Fr = 0.198 (Top Left), (b) DTMB 5415 Original Hull at Fr = 0.198 (Bottom Left)

Figure 12 presented the comparison of the wave patterns at the lowest tested speeds using dynamic pressure contours. At the lower speed (Fr = 0.198), the flow directed by the FlowBow® configuration (Figure 12A) increased pressure resistance, since a stable pressure distribution had not yet formed around the device. This results in flow accumulation, particularly at the leading edge and near the trailing region, as indicated by localized high-pressure concentrations. A comparable condition is observed in the original DTMB 5415 hull (Figure 12B), although the pressure distribution remains more symmetric and less effectively redistributed.

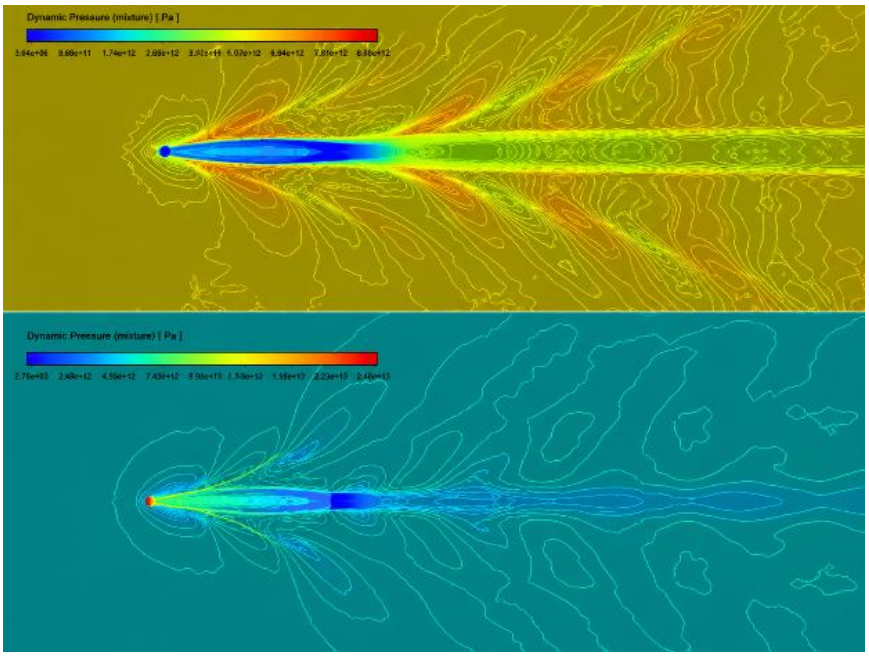

Figure 13. Wave Contour Distributions at Two Froude Numbers for Different Bow Configurations: (a) FlowBow® at Fr = 0.352 (top), (b) DTMB 5415 Original Hull at Fr = 0.352 (Bottom Right).

Figure 13 presented the comparison of the wave patterns at the highest tested speeds using dynamic pressure contours FlowBow® contribute to lateral release of pressure which contributes to a reduction in wave making resistance. At the higher speed (Fr = 0.352), the DTMB 5415 model equipped with FlowBow® exhibits a distinct flow region that is redirected laterally as it passes the trailing edge, as shown in Figure 13a. This behavior contrasts with the bulbous bow configuration (Figure 13b), where, despite some lateral flow, pressure remains concentrated around the bow region. The localized accumulation of high-pressure zones, indicated by the red contours, suggests increased wave-making resistance [18].

CONCLUSION

The DTMB 5415 design incorporating the FlowBow® was developed in accordance with the design specifications outlined in the FlowBow patent and ensures that the volume and submerged volume parameters match those of the DTMB 5415 ship model. CFD testing on the DTMB 5415 ship model was validated, with the difference in drag results compared to EFD testing remaining below 5% across all speed variations. These results were used as the basis for analyzing the drag of the existing DTMB 5415 ship and the DTMB 5415 ship with FlowBow®. The addition of FlowBow® to the DTMB 5415 successfully reduced the ship's resistance at speeds beyond a Froude number of 0.249, with the greatest reduction observed in the study occurring at the highest test speed (Fr = 0.352), amounting to 8.57%.

ACKNOWLEDGEMENT

The authors also extend gratitude to Indonesian National Research and Innovation Agency (BRIN) and West Japan Fluid Engineering Laboratory for the experimental data.

REFERENCES

[1] Y. Y. E. Darma, R. A. . Sugiarto, A. F. N. Oloan, and F. Narotama, "CFD-Based Comparative Study of Axe Bow and Bulbous Bow Designs for Corvette Warship Deployment in Natuna Waters", *IJMEIR*, vol. 10, no. 3, pp. 827–837, Sep. 2025. doi: https://doi.org/10.12962/j25481479.v10i3

[2] Samuel S., Sam Timoty Frans Evan S., Trimulyono A., Muhammad Iqbal. (2022). An analysis of the effect of the bow entrance angle on ship resistance. doi: http://doi.org/10.22441/sinergi.2022.2.011

[3] Papanikolaou, A. (2014). Ship design: Methodologies of preliminary design. In Ship Design: Methodologies of Preliminary Design. Springer Netherlands. doi: https://doi.org/10.1007/978-94-017-8751-2

[4] Zhang, Y., et al. (2021). CFD-based optimization of bulbous bow for resistance reduction. Ocean Engineering.

[5] Deng, R., Huang, S., Wang, S., Liu, H., Yu, X., & Wu, T. (2023). Experimental study on the influence of a T-foil and bulbous bow on the resistance and motion in regular head waves of trimarans. Ocean Engineering. doi: 10.1016/j.oceaneng.2023.114990

[6] Gaggero, S., et al. (2021). CFD prediction of ship resistance and propulsion performance. Applied Ocean Research.

[7] Flowbow. (2023). Flowbow. Retrieved May 24, 2024, from https://www.flowbow.no/

[8] M. G. Hutabarat, S. Samuel, and A. Trimulyono, "Analisis pengaruh variasi bentuk haluan dan buritan terhadap hambatan pada kapal US Navy Combatant DTMB Model 5415 dengan metode CFD [Analysis of the influence of variations in the shape of the bow and stern on the resistance of the US Navy Combatant DTMB Model 5415 ship using the CFD method] ," *Jurnal Teknik Perkapalan*, vol. 12, no. 2, Jun. 2024. [Online]. Retrieved from : https://ejournal3.undip.ac.id/index.php/naval/article/view/44992/0

[9] Suastika, K. (2023). Dinamika Fluida Komputasi. itspress.

[10] Menter F R. (1994). Two-equation eddy-viscosity turbulence models for engineering applications AIAA Journal 32 1598–605

[11] Putra, Z. T. S. (2020). Analisis Hambatan Pada Kapal Katamaran Dengan Transverse Stepped Hull Dengan Metode Computational Fluid Dynamics [Resistance Analysis on Catamaran Ships with Transverse Stepped Hull Using Computational Fluid Dynamics Method]. http://repository.its.ac.id/id/eprint/80253

[12] ITTC. (2011). Practical Guidelines for Ship CFD Applications.
[13] Versteeg, H. K., & Malalasekera, W. (2007). An introduction to computational fluid dynamics: The finite volume method (2nd ed.). Pearson Education.
[14] Regitasyali, S., Aliffrananda, M. H. N., Hermawan, Y. A., Hakim, M. L., & Utama, I. K. A. P. (2022). Numerical investigation on the effect of homogenous roughness due to biofouling on ship friction resistance. IOP Conference Series: Earth and Environmental Science, 972(1). doi: https://doi.org/10.1088/1755-1315/972/1/012026
[15] Dewantara, D. R., & Utama, I. K. A. P. (2025). The Performance of Wing-In-Ground Craft with Anhedral and Rear Planform Cropping Wing Configurations.
[16] Celik I B, Ghia U, Roache P J, Freitas C J, Coleman H and Raad P E. (2008). Procedure for Estimation and Reportingof Uncertainty Due to Discretization in CFD Applications J. Fluids Eng. 130 078001
[17] Suryawan, D., Suastika, I. K., & Ali, B. (2025). Comparative study of ship resistance calculated from CFD and obtained from towing tests: Case study of LCT vessel. IOP Conference Series: Earth and Environmental Science, 1461(1). doi: https://doi.org/10.1088/1755-1315/1461/1/012006
[18] Yasin Öztürk, M., & Çoşgun, T. (2024). Impact of Bulbous Bow Geometry on Ship Resistance: A Numerical Study. In International Journal of Advanced Natural Sciences and Engineering Researches (Vol. 11, Issue 11). doi; https://as-proceeding.com/index.php/ijanser